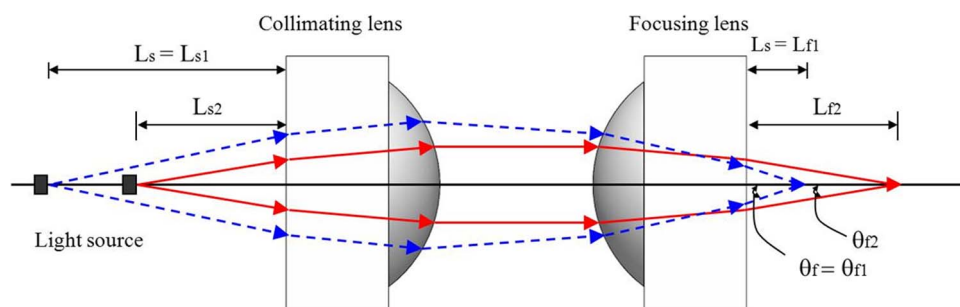


Design of an Alignment Tolerant Miniature Optical Subassembly Module

Volume 6, Number 2, April 2014

Hak-Soon Lee
Wenjing Yue
Sang-Shin Lee



DOI: 10.1109/JPHOT.2014.2309644
1943-0655 © 2014 IEEE

Design of an Alignment Tolerant Miniature Optical Subassembly Module

Hak-Soon Lee, Wenjing Yue, and Sang-Shin Lee

Department of Electronic Engineering, Kwangwoon University, Seoul 139-701, Korea

DOI: 10.1109/JPHOT.2014.2309644

1943-0655 © 2014 IEEE. Translations and content mining are permitted for academic research only. Personal use is also permitted, but republication/redistribution requires IEEE permission.

See http://www.ieee.org/publications_standards/publications/rights/index.html for more information.

Manuscript received January 24, 2014; accepted February 26, 2014. Date of publication March 4, 2014; date of current version March 13, 2014. This work was supported by a National Research Foundation of Korea (NRF) grant funded by the Korean government (MSIP) (No. 2013-008672) and by a research grant from Kwangwoon University in 2014. Corresponding author: S.-S. Lee (e-mail: slee@kw.ac.kr).

Abstract: A miniature optical subassembly module incorporating a pair of collimating and focusing lenses was proposed and designed to provide affordable alignment tolerance in terms of optical coupling efficiency. The light source was specifically modeled taking advantage of multiple point sources placed on the emitting aperture. This scheme was practically verified to be superior to the conventional scheme involving a single point source by estimating the focal length and spot size of a focused beam. The performance of the proposed source modeling was scrutinized with respect to the number of point sources. The optical coupling of the subassembly to a fiber was investigated theoretically and experimentally in light of the characteristics of the displacement of the focused beam relative to the lateral displacement of the light source. Finally, a tradeoff between the positional 3-dB tolerance of the light source and the maximum available coupling efficiency was established with certitude.

Index Terms: Micro-optics, optical interconnects, fiber optic systems, applications, theory and design.

1. Introduction

Demand for cost-effective short reach communications has been growing tremendously due to the need to efficiently deliver a large volume of information content, including video, audio, and data, to and from diverse consumer electronic devices, such as smartphones, smart TVs, digital media players, etc. Recently an active optical interconnect (AOI) has emerged as a viable candidate to substitute conventional copper based cables [1]–[11]. Most of the previous AOI approaches, drawing upon an optical subassembly module requiring active monitoring, are not attractive in terms of the cost, manufacturing time, and productivity [3]–[6]. In an effort to overcome these issues a passively assembled optical subassembly module has been actively researched [7]–[11]. The structural tolerance, which is directly relevant to the cost and optical coupling efficiency, is known to be principally governed by the alignment of a light source [11]. In this paper, we have investigated the implementation of a passively-aligned, compact, transmission optical subassembly module in terms of the positional tolerance of the light source. The research was undertaken with the assistance of both ray-tracing based simulation and an experiment. A modeling scheme, where the light source is approximated to consist of multiple point sources rather than a single source, was primarily proposed and assessed. Finally, the overall positional tolerance of the light source belonging to the subassembly module was quantitatively explored with respect to the peak optical coupling efficiency.

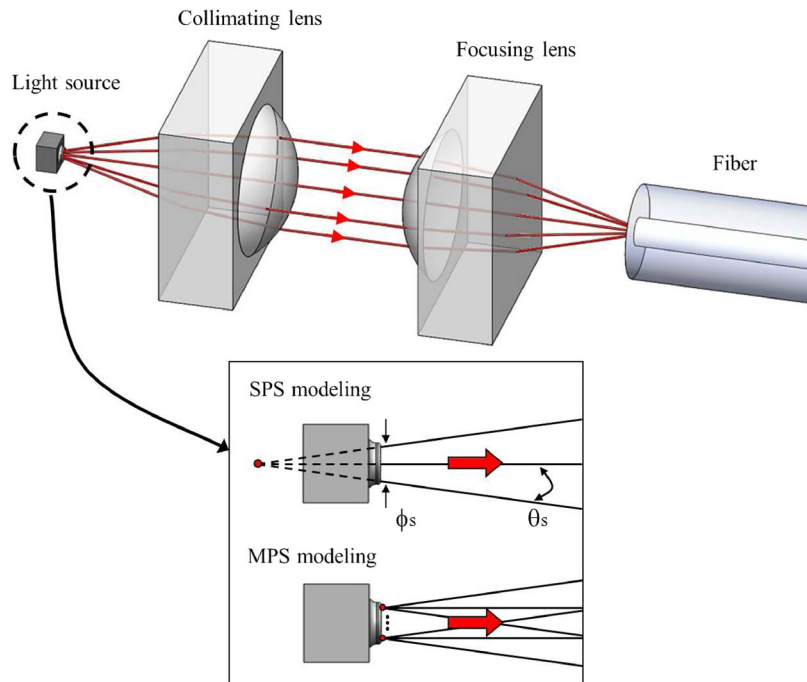


Fig. 1. Proposed lens based optical subassembly module, with light source modeling included.

2. Proposed Compact Optical Subassembly Module

The configuration of an optical subassembly module of interest, which involves a light source, a receiving fiber, and a beam-coupling optics comprising collimating and focusing lenses, is sketched in Fig. 1. The light beam generated by the source is collimated and then focused to reach the fiber. In order to precisely study the overall structural tolerance of the module, the light source should be appropriately modeled, as depicted in Fig. 1. In the case where there is a light source with an emitting aperture of ϕ_s and a divergence angle of θ_s , the source had previously been simplistically treated as a single point source (SPS) positioned behind the aperture so as to provide a beam with the corresponding beam spot and divergence [12]–[14]. Taking into account the fact that a multi-mode field profile instead of a single-mode profile is obtained depending on the dimension of the aperture and index contrast, we attempted to emulate the source utilizing a multi-point source (MPS). This MPS method was particularly evaluated by observing the focal length and spot size of the focused beam when the aperture and position of the light source and its distance to the collimating lens varied. The performance of the method was then investigated in terms of the number of point sources involved in the modeling.

The relationship between the coupling efficiency and the alignment tolerance associated with the source is addressed here. As can be seen in Fig. 2(a), the ray coming out of the focusing lens is guaranteed to be captured by the fiber as long as the propagation angle θ_f is smaller than the angle of acceptance θ_{fA} corresponding to the numerical aperture (NA_f) of the fiber. Fig. 2(b) describes the effect of both the light source-to-collimating lens distance and the focal length upon the propagation angle of the focused beam θ_f . The angle θ_f decreases from θ_{f1} to θ_{f2} when the source-to-lens distance L_s decreases from L_{s1} to L_{s2} , while, accordingly, the focal length of the focused beam lengthens from L_{f1} to L_{f2} . The impact of the lateral displacement of the light source upon the fiber coupling is described in detail in Fig. 2(c). It is thought that the alignment tolerance is predominantly determined by the displacement of the focused beam relative to the lateral source misalignment, $\Delta D \equiv -D_f/D_s = -\sqrt{d_{fx}^2 + d_{fy}^2} / \sqrt{d_{sx}^2 + d_{sy}^2}$, which can be approximated as the ratio of L_s to L_f [15]. The fact that ΔD assumes a negative value means that the displacement of the light source and

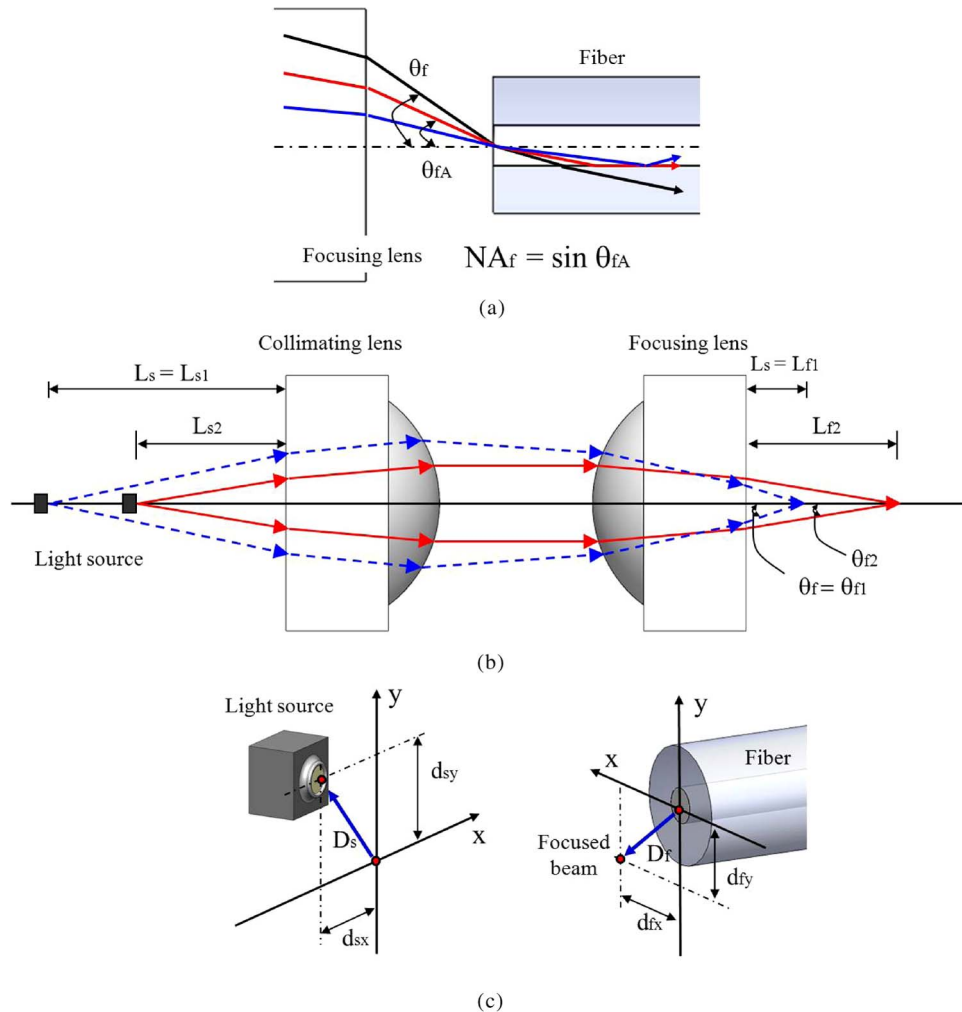


Fig. 2. (a) Coupling to an optical fiber with an angle of incident beam. (b) Effect of the longitudinal displacement of the light source on the focused beam. (c) Effect of the lateral displacement of the light source on the focused beam.

focused beam are opposite in direction. The optical coupling efficiency will be affected as a result of the lateral source displacement.

3. Characterization of the Optical Subassembly Module

Crucial design issues relevant to the optical subassembly module were first examined with the use of a ray-tracing technique, referring to structural parameters provided in Fig. 3. The light source operates at an 850-nm wavelength, while a 2.5-mm thick aspheric lens made up of polycarbonate ($n = 1.586$) is used for beam collimation and focusing. Both the collimating lens and the focusing lens are designed to have the same structural parameters, including a radius of 1.48 mm, a conic constant of -0.26 , and 4th, 6th and 8th coefficients of 0.82×10^{-2} , 0.25×10^{-2} , and 0.10×10^{-2} , respectively. The gap between the two lenses is set at 0.4 mm. In order to conduct a practical characterization of the module, as displayed in Fig. 4, a lens-based coupling optics with a footprint of $5.4 (L) \times 8 (W) \times 5 (H) \text{ mm}^3$ was prepared via plastic injection molding. The light beam is captured by use of a beam profiler linked to a CCD camera. In this work, two types of fibers with large and small cores of 62.5 and 9 μm were employed to serve as the light source exhibiting different apertures and divergence characteristics. As presented in Fig. 5, the beam profile and spot

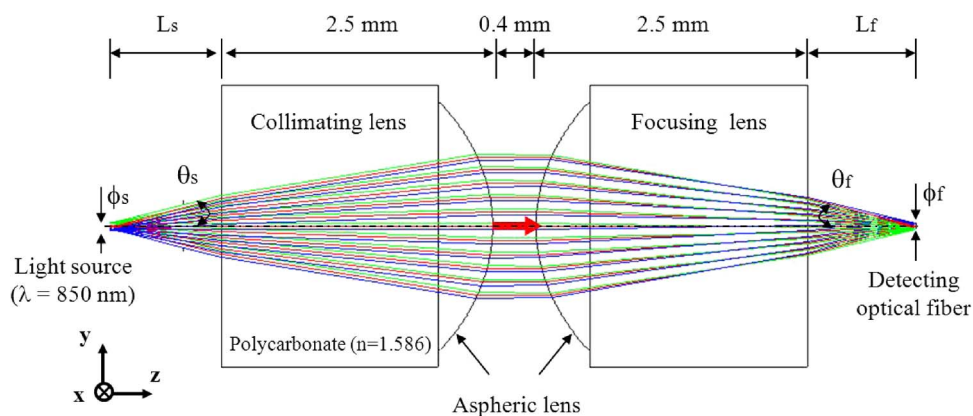


Fig. 3. Ray tracing based design of the proposed subassembly module.

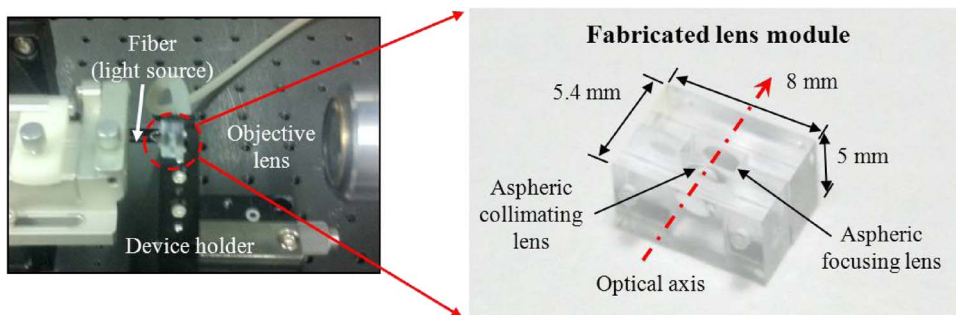


Fig. 4. Manufactured lens module used for characterizing the proposed subassembly module.

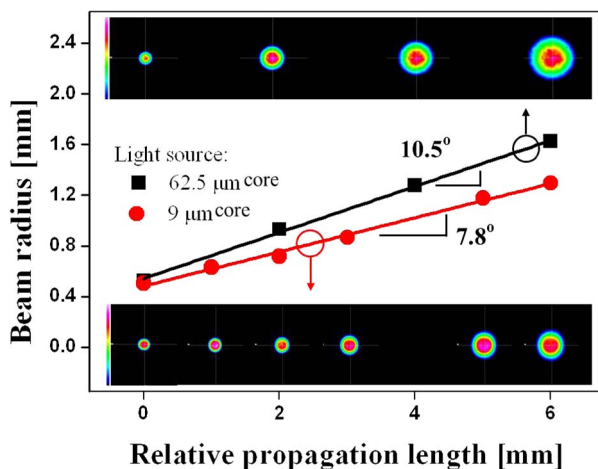


Fig. 5. Observed beam propagation of two different fiber based light sources.

size were initially monitored as a function of the propagation distance to obtain divergence angles of 10.5° and 7.8° for the 62.5 and 9 μm sources, respectively.

First, we studied the dependence of the proposed MPS modeling scheme on the number of point light sources, which are assumed to be collinearly positioned with equidistant intervals on the surface of the source aperture. For different source-to-lens distances ranging from 0.6 to 1.4 mm, in

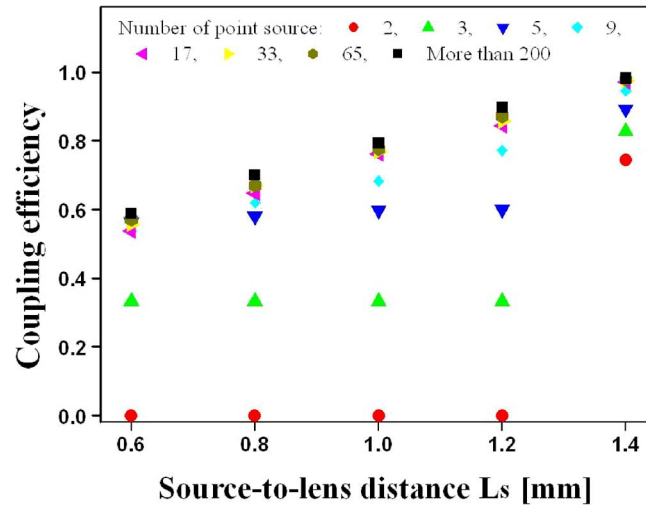


Fig. 6. Calculated dependence of the proposed MPS modeling scheme on the number of point light sources for different source-to-lens distances.

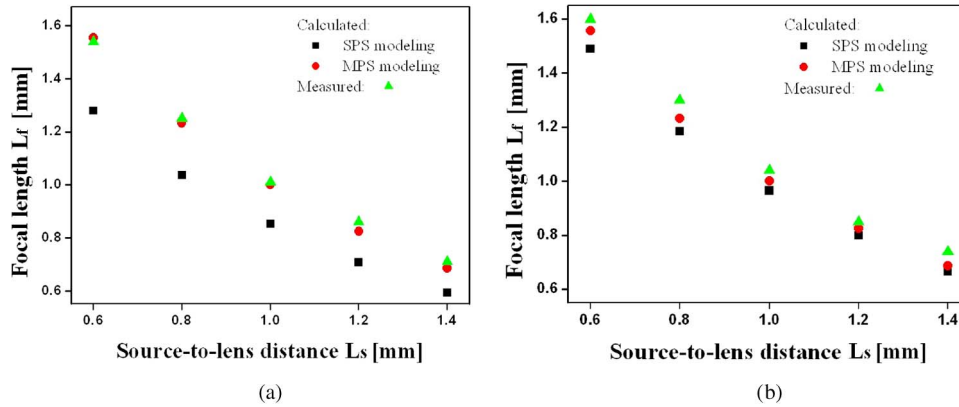


Fig. 7. Estimation of the focal length based on the source modeling schemes of MPS and SPS (a) for a large $62.5\text{-}\mu\text{m}$ source and (b) for a small $9\text{-}\mu\text{m}$ source.

the case of the large light source, optical coupling to a detector with a $50\text{-}\mu\text{m}$ aperture via the lens pair was observed by increasing the number of point sources from 2 to over 200. As shown in Fig. 6, the coupling efficiency tends to converge to a final value as the number of point sources increases, which may be available from a seamlessly packed surface light source. From practical applications of the proposed model, the interval between two adjacent point sources on top of the aperture was determined to be below $\sim 1\ \mu\text{m}$. In this respect, we have conducted simulations adopting more than 65 and 11 point sources for large and small sources of 62.5- and $9\text{-}\mu\text{m}$ apertures, respectively.

To undertake an efficient comparison of the proposed MPS and conventional SPS modeling schemes, the dependence of the position and spot size of the focused beam upon the source-to-lens distance L_s was specifically explored. Fig. 7(a) and (b) shows the focal length for the large and small sources with 62.5- and $9\text{-}\mu\text{m}$ apertures, respectively, when L_s varies from 0.6 to 1.4 mm in steps of 0.2 mm. For the large source, the discrepancy between the calculation and experiment was less than 0.02 mm for the MPS modeling but as big as 0.2 mm for the SPS case. For the small source, the differences of concern were approximately less than 0.04 mm and greater than 0.1 mm for the MPS and SPS schemes, respectively. Fig. 8 shows the focused spot size for the large and small sources. When L_s ranged from 0.6 to 1.4 mm, in the case of the large source, the difference

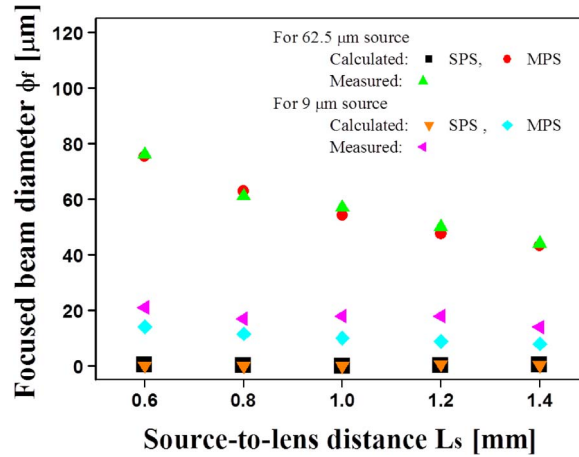


Fig. 8. Focused beam spot size with the source-to-lens distance.

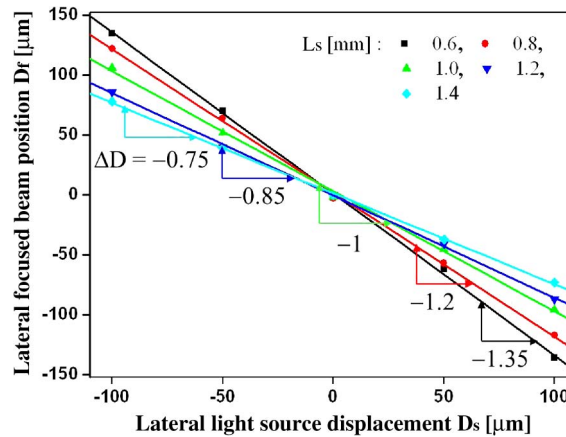


Fig. 9. Calculated relative displacement of the focused beam ΔD obtained from the relationship between the lateral displacements of the light source and focused beam, for different source-to-lens distances.

between the estimated and demonstrated beam diameters was found to be greater than $40 \mu\text{m}$ and less than $1 \mu\text{m}$ for the SPS and MPS models, respectively. For the small source, the corresponding differences were greater than $13 \mu\text{m}$ and less than $6 \mu\text{m}$ for the SPS and MPS models, respectively. Consequently, these results showed that the proposed MPS model is obviously superior to the conventional SPS scheme.

Tapping into the proposed MPS-based source modeling, we looked into the alignment tolerance associated with the lens based optical subassembly module in terms of the optical coupling. For the lens pair used in this study, the dependence of the relative displacement of the focused beam ΔD on the source-to-lens distance L_s was calculated by observing the slope for an approximately linear relationship between the lateral source displacement and focused beam displacement, as plotted in Fig. 9. For each of the cases of L_s ranging from 0.6 to 1.4 mm, the focused beam position was recorded when the light source was displaced from -100 to $100 \mu\text{m}$ in steps of $50 \mu\text{m}$. ΔD was observed to vary from -1.35 to -0.75 when L_s changed from 0.6 to 1.4 mm. Next, the angle of the focused beam θ_f was monitored as a function of the relative displacement of the focused beam position ΔD . As plotted in Fig. 10, when ΔD was altered from -1.35 to -0.75 , for the large source, the angle increased from 7.6° to 13.4° in the calculation and from 7.3° to 12.3° in the experiment. In

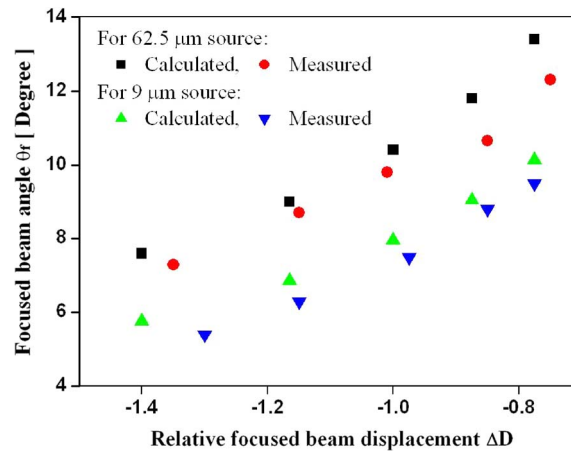


Fig. 10. Angle of the focused beam with the relative displacement of the focused beam ΔD .

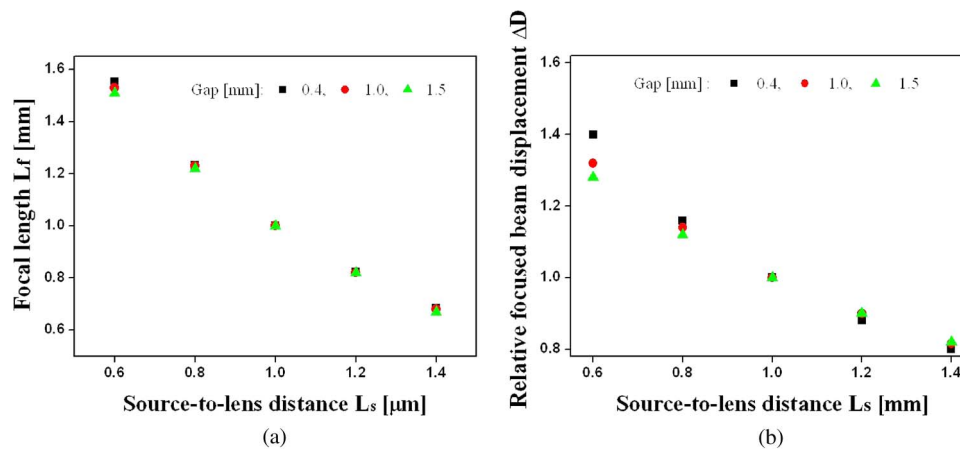


Fig. 11. Influence of the gap between the collimating and focusing lens on (a) focal length with the source-to-lens distance and (b) relative focused beam displacement with the source-to-lens distance.

the case of the small source, the calculated and measured angles increased from 5.8° to 10.2° and from 5.4° to 9.5° , respectively. Overall, a good correlation between the simulation and the experiment was achieved. It is stated that the angle of the focused beam θ_f increased with diminishing ΔD so as to degrade maximum available coupling efficiency, indicating that a tradeoff exists between the alignment tolerance and peak optical coupling.

Then, we explored the effect of the gap between the collimating and focusing lens on the focal length and relative focused beam displacement with the source-to-lens distance L_s , for the proposed MPS modeling. As shown in Fig. 11(a), the focal length hardly changed in response to a variation in L_s from 0.6 to 1.4 mm for gaps of 0.4, 1.0, and 1.5 mm. As can be seen in Fig. 11(b), however, ΔD exhibited increasing sensitivity to the gap with decreasing L_s , as anticipated. Therefore, the gap should be adaptively taken into account when ΔD is controlled by adjusting L_s .

Finally, in order to identify the tradeoff between the alignment tolerance of the light source and the maximum available coupling efficiency, we attempted to couple light to a graded index plastic optical fiber with a numerical aperture of ~ 0.185 and a core of $62.5 \mu\text{m}$ in diameter [16], with respect to large and small sources. Fig. 12 plots the relationship between the peak fiber coupling efficiency and the lateral alignment tolerance of the light source. The maximum coupling was first checked

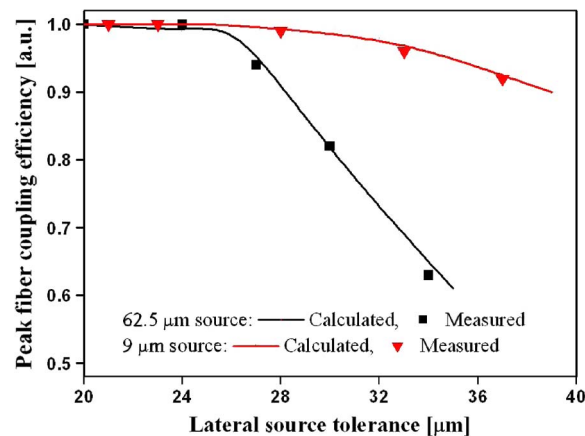


Fig. 12. Observed relationship between the peak fiber coupling efficiency and the 3-dB alignment tolerance for the large and small light sources.

when L_s varied from 0.6 to 1.4 mm in increments of 0.2 mm. For a constant value of L_s , the optical power coupled to the fiber was monitored as the source was displaced laterally in incremental steps of 10 μm . The corresponding 3-dB alignment tolerance was estimated by discovering the displacement, which caused the optical output to decline to half of the peak optical output. For the large source the coupling efficiency dropped by an amount of approximately 37% when the tolerance was extended from 20 to 34 μm . For the small source, the coupling decreased by $\sim 7\%$ as the tolerance was extended from 20 up to 37 μm . In regard to the optical coupling, the large source exhibited higher sensitivity to the tolerance than that of the small source, on account of its larger divergence. It is thus asserted that to enhance the coupling efficiency for constant positional tolerance, it is preferred for the light source to have smaller divergence. The results relating to the alignment tolerance for a given peak coupling efficiency will play a vital role in designing transmission and reception modules.

4. Conclusion

A miniature optical subassembly module based on a pair of collimating and focusing lenses was designed and analyzed theoretically and experimentally in terms of the relationship between the alignment tolerance of the light source and the coupling efficiency. The light source was specifically modeled by utilizing an MPS scheme instead of the conventional SPS scheme, thus enhancing the accuracy of the module design. The sensitivity of the optical coupling to the source alignment was keenly investigated by introducing the focused beam displacement relative to the source displacement under various conditions. The tradeoff between peak optical coupling and the light source alignment tolerance was ultimately identified and later will be applied to build a variety of passive alignment-based optical subassembly modules for receivers and transmitters.

References

- [1] D. A. B. Miller and H. M. Ozaktas, "Limit to the bit-rate capacity of electrical interconnects from the aspect ratio of system architecture," *J. Parallel Distrib. Comput.*, vol. 41, no. 1, pp. 42–52, Feb. 1997.
- [2] D. A. B. Miller, "Physical reasons for optical interconnection," *Int. J. Optoelectron.*, vol. 11, no. 3, pp. 155–168, May/June. 1997.
- [3] S. C. Liu, R. R. Liu, W. P. Chen, C. Z. Wu, and J. S. Pan, "Optical sub-assembly solution for single fiber optical HDMI connector," in *Proc. SPIE*, 2009, vol. 7229, pp. 722906-1–722906-10.
- [4] G. C. Boisset, B. Robertson, and H. S. Hinton, "Design and construction of an active alignment demonstrator for a free-space optical interconnect," *IEEE Photon. Technol. Lett.*, vol. 7, no. 6, pp. 676–678, Jun. 1995.
- [5] K. Ishikawa, J. Zhang, A. Tuantranont, V. M. Bright, and Y. C. Lee, "An integrated micro-optical system for VCSEL-to-fiber active alignment," *Sens. Actuators A, Phys.*, vol. 103, no. 1/2, pp. 109–115, Jan. 2003.
- [6] R. Zhang, J. Guo, and F. G. Shi, "Fast fiber-laser alignment: Beam spot-size method," *J. Lightw. Technol.*, vol. 23, no. 3, pp. 1083–1087, Mar. 2005.

- [7] R. A. Boudreau and S. M. Boudreau, *Passive Micro-Optical Alignment Methods*. New York, NY, USA: Taylor & Francis, 2005.
- [8] E. Palen, "Low cost optical interconnects," in *Proc. SPIE*, 2007, vol. 6478, pp. 6478-041–6478-045.
- [9] H. S. Lee, J. Y. Park, S. M. Cha, S. S. Lee, G. S. Hwang, and Y. S. Son, "Ribbon plastic optical fiber linked optical transmitter and receiver modules featuring a high alignment tolerance," *Opt. Exp.*, vol. 19, no. 5, pp. 4301–4309, Feb. 2011.
- [10] S. H. Hwang, J. W. Lim, and B. S. Rho, "Simple and high-accuracy integration for parallel optical subassembly with 120-Gbits/s data transmission," *Opt. Eng.*, vol. 49, no. 9, pp. 095401-1–095401-6, Sep. 2010.
- [11] J. Y. Park, H. S. Lee, S. S. Lee, and Y. S. Son, "Passively aligned transmit optical sub-assembly module based on a WDM incorporating VCSELs," *IEEE Photon. Technol. Lett.*, vol. 22, no. 24, pp. 1790–1792, Dec. 2010.
- [12] J. Zhang, P. V. Ramana, J. Chandrappan, C. W. Tan, Y. Y. Chai, Y. M. Khoo, W. L. Teo, J. L. Shing, T. Wang, and V. M. Ramkumar, "Development of optical subassembly for plastic optical fiber transceiver in high-speed applications," *IEEE Trans. Adv. Packag.*, vol. 33, no. 2, pp. 428–432, May 2010.
- [13] W. Hao, H. Zhangdi, Y. Ziyang, Q. Xiaoshi, X. Fei, C. Beckham, and L. Yanqing, "Aberration analysis and efficiency improvement of a bidirectional optical subassembly," *Opt. Eng.*, vol. 48, no. 10, pp. 105008-1–105008-6, Oct. 2009.
- [14] J. M. Trewhella, M. M. Oprysko, H. Backhauss, M. Ritter, and M. Cina, "Unibody plastic injection-molded optical sub-assembly for large core fiber," in *Proc. Electron. Compon. Technol. Conf.*, 1996, pp. 1116–1121.
- [15] E. Hecht, *Optics*, 4th ed. Reading, MA, USA: Addison Wesley, 2002.
- [16] Plastic Optical Fiber, Chromis Fiberoptics Co., USA